Origins of the Speckles and Slow Dynamics of Polymer Gels

To Ngai,[†] Chi Wu,*[,†,‡] and Yun Chen[§]

Department of Chemistry, The Chinese University of Hong Kong, Shatin. N.T., Hong Kong, The Open Laboratory of Bond Selective Chemistry, Department of Chemical Physics, University of Science and Technology of China, Hefei, Anhui, China, and Department of Chemical Engineering, National Cheng Kung University, Taiwan, 70101

Received: August 19, 2003

The [2+2] photocycloaddtion of 7-methacryloyloxy-4-methylcoumarin attached to the PMMA chain can transfer a semidilute solution to a homogeneous and speckle-free chemical gel with some "extraordinary" dynamics. First, its normalized intermediate scattering function $f(q,\tau)$ can fully relax to zero, indicating that the gel has no frozen-in static component. This supports our previous conclusion that the speckles of polymer gels originates from large voids inside, not cross-linked chains (clusters). Second, $f(q,\tau)$ consists of a fast and a slow relaxation. Both of them are nondiffusive. For the fast mode, there is nearly no change in its decay rate as well as its related scattering intensity during the sol−gel transition, but for the slow mode, the relaxation slows down and its related scattering intensity sharply increases $\sim 10^2$ times. The alternative analysis of the measured time correlation function by the partial heterodyne method leads to only one relaxation rate, similar to that of the slow mode. Our results confirm that the fast mode is related to the well-known motions of subchains (blobs) between two cross-linked points and reveal that the slow relaxation is due to thermally agitated density fluctuation of the gel network. In comparison with its corresponding semidilute solution, the cross-linking makes the motions of different blobs more correlated, and at the same time, reduces the dimension (static correlation length) of the density fluctuation and slows down its relaxation rate.

Introduction

A polymer gel can be roughly considered as a three-dimensional cross-linked network of chains swollen with a large amount of solvent. It normally has a much more complicated structure and dynamics in comparison with a corresponding polymer solution. It has a coexisting solid-like and liquid-like behavior.[1,2] Polymer gels can be neutral or ionic and further grouped as chemical or physical gels, depending on whether the cross-linking is made of covalent bonds or physical interaction, such as hydrogen bonding, electrostatic interaction, and hydrophobic association. Normally, chemical gelation is irreversible, while physical gelation could be reversible by alternating temperature, solvent composition, pH, or ionic strength.[3] Typical chemical gels are prepared by conventional radical copolymerization of monomers and cross-linking agents. It is helpful to note that the choice of a proper pair of monomer and cross-linking agent with a similar chemical structure and reactivity to avoid an inhomogeneous distribution of the cross-linking points is rather difficult, if not impossible. Chemical gels can also be prepared from polymer solutions by γ-irradiation or by attaching cross-linkable groups, such as double bonds, to the chain backbone.[4]

The study of the sol−gel transition is a long-standing old problem. Laser light scattering (LLS) as a nondestructive method has been widely used.[5−9] Chemical gels normally are heterogeneous and nonergodic in LLS, i.e., the time-averaged scattering intensity $\langle I\rangle_T$ at one sample position is different from the ensembly-averaged scattering intensity $\langle I\rangle_E$ over different sample positions. Tanaka et al.[10] showed that the intensity−intensity time correlation function $G^{(2)}(\tau)$ [$\equiv\langle I(0)I(\tau)\rangle$] of chemically cross-linked poly(acrylamide) gels measured in dynamic LLS followed a single exponential decay despite that the length of the chain segment between two neighboring cross-linking points was broadly distributed. They attributed it to the cooperative nature of the polymer network swollen in solvent. Such a single-exponential decay is not universal because gels normally contain large static frozen-in components, reflecting the decrease of the intercept of the baseline-normalized $G^{(2)}(\tau)$, i.e., $g^{(2)}(\tau)$ [$\equiv(\langle I(0)I(\tau)\rangle - \langle I(0)\rangle^2)/\langle I(0)\rangle^2$] at $\tau \rightarrow 0$, as the cross-linking proceeds. In addition, gels often contain a sol fraction, i.e., individual uncross-linked chains.

To name but a few, Munch et al.[11] found that $g^{(2)}(\tau)$ follows a double-exponential decay in the free radical copolymerization of styrene and divinylbenzene in benzene. They interpreted the fast and slow decays, respectively, as the fluctuation of cooperative concentration and the diffusion of large polymer clusters. Adam et al.[6] reported that $g^{(2)}(\tau)$ could be fitted by a stretched exponential decay for the gelation of polyurethane when the polymer concentrations were lower than a critical value of 7 v/v%, but became a power law dependence of the delay time τ at higher concentrations. Martin et al.[7,8] also observed a similar exponential decay for silica and epoxy gels and a power law function of $g^{(2)}(\tau)$ at and after the gelation threshold. It is generally recognized that the fast decay is related to the diffusive relaxation of chain segments in the maze of other chains, but the slow decay is less understood. It is necessary to note that the study of the dynamics during a copolymerization-induced sol−gel transition is rather messy because the polymer concentration, the chain length, and the branching extent increase during the reaction, which makes the study under an extremely poorly defined condition. Moreover, most of the past LLS

* Corresponding author. Department of Chemistry, The Chinese University of Hong Kong, Shatin. N.T., Hong Kong.
† The Chinese University of Hong Kong.
‡ University of Science and Technology of China.
§ National Cheng Kung University.

10.1021/jp0309926 CCC: $27.50
Published on Web 04/14/2004

studies before Pusey and Megen[12] did not consider seriously the inhomogeneity of polymer gels.

The structural inhomogeneity of polymer gels was generally attributed to the localization of chain segments in space due to the cross-linking,[13,14] i.e., the formation of clusters with some limited motions around their fixed average positions. It has been considered as an *intrinsic* property of a polymer gel network. One obvious characteristic is the appearance of speckles; namely, a significant variation of the scattering intensity with the sample position at which the incident light hits.[15−17] In this way, the scattering intensity from a gel contains static and dynamic contributions. The static part comes from inhomogeneous frozen-in components (we do not discuss its nature at this moment), independent of time, while the dynamic part was attributed to diffusive relaxation.[18−21] The concept of nonergodicity, stated by Pusey and Megen,[12] has led to the development of several relevant methods for the study of dynamics of polymer gels, such as the partial heterodyne and intermediate scattering function analysis.[22−24] More recently, Shibayama et al.[25,26] showed that the spatial inhomogeneity also exists in physical gels and revealed that the structure inhomogeneity strongly depends on the gelation process and experimental conditions.[27−31] This leads to a question whether the speckles are really intrinsic.

If the speckles are due to the existence of frozen-in cross-linked chains (clusters), they must be fairly large and inhomogeneously distributed inside. However, typical sizes of polymer clusters measured near the gelation threshold are normally in the range of $\sim 10^2-10^3$ nm, much smaller than the a typical dimension of the LLS scattering volume ($\sim 200\ \mu$m). In addition, we found several interesting experimental facts in the literature; namely, the inhomogeneity increases with the amount of the cross-linking agent, the reaction rate, and the swelling extent.[16] In principle, we should observe the opposite effects, i.e., more cross-linking agents should make the polymer clusters more uniform and the swelling would result in a more homogeneous gel network. Moreover, it is rather difficult to explain why the scattering intensity increases as the gel swells and as the solvent quality decreases if we attribute the origin of the speckles to the existence of static frozen-in polymer clusters.

Recently, we utilized the swelling of thermally sensitive narrowly distributed spherical poly(*N*-isopropyl-acrylamide) microgels to imitate the growing of polymer clusters nearby the gelation threshold.[31] The swelling of billions of such microgels in a dispersion can change a flowing liquid into a macroscopically immobile hybrid gel. The size of these uniform microgels can vary in the range 45−110 nm, depending on the dispersion temperature. We found that the inhomogeneity of the resultant gel increases with an increasing swelling rate. Moreover, the hybrid gel can become homogeneous and speckle-free when the microgels are closely packed under centrifugation before their swelling. Note that the microgels, even in the swollen state, are smaller than the wavelength of the laser light used. The scattering volume contains $\sim 10^9$ microgels. Therefore, the speckles (inhomogeneity) cannot be related to a possible uneven distribution of polymer clusters inside. Our results indicate that the inhomogeneity is actually due to large voids inside the gel. It is understandable that large voids are formed if the growing rate of polymer clusters is much higher than their relaxation rates (diffusion). This is because there is no sufficient time for them to relax to their equilibrium positions so that they are "frozen" (jammed) in space. The voids (spaces) between polymer clusters are much larger than the mesh size between cross-linked chains inside the microgels.

It is helpful to note that before reaching the gelation threshold, the gelation system often becomes or is a semidilute solution. It is well known that, in addition to a fast diffusive mode, there also exists a slow relaxation in semidilute solution. The fast mode is well understood and attributed to the motions of the subchains (blobs) between two entangled points. However, the nature of the slow relaxation and how it is related to the slow dynamics inside a gel network have not been satisfactorily addressed. One of the reasons is because the gel inhomogeneity complicates such a study. It would be ideal if we could prepare a uniform gel network and then study the gel dynamics (relaxations) without any interference of the inhomogeneity. Moussaid et al.[30] showed that the gels made of charged poly(acrylic acid) (PAA) have little or no excess scattering in comparison with their corresponding solutions. However, it is known that introducing charged groups into polymer chains would greatly complicate the gel dynamics because of long-range electrostatic interaction.

In the past, various groups have claimed that their gels were full relaxable by showing a complete decay of the measured $g^{(2)}(\tau)$.[30,32] Unfortunately, the intensity of the light scattered from static frozen-in components $\langle I_s \rangle_T$ was wrongly taken as part of the baseline in the normalization of $G^{(2)}(\tau)$. Such a mistake is evident from the decrease of the measured intercept $g^{(2)}(\tau \rightarrow 0)$ during the gelation. In other words, these measurements were not completely homodyne in which static frozen-in components actually acted as local oscillators. There is no question that cross-linked polymer chains cannot move a long distance inside a gel. However, it is helpful to note that in dynamic LLS the excursion of the scattering object over a distance of $1/q$ ($\sim$100 nm) is sufficient to lead to a complete decay of $g^{(2)}(\tau)$. Later, we will show that the cross-linked chains can undergo such an excursion over a length scale of $1/q \sim 100$ nm around their equilibrium positions, further confirming that the static frozen-in components are not the cross-linked chains (clusters), but large voids inside. We will discuss this later.

Recently, we have prepared linear copolymer poly(methyl methacrylate-*co*-7-methacry-loyloxy-4-methylcoumarin) [P(MMA-*co*-AMC)] chains because two coumarin groups can undergo the [2+2] photocycloaddition under UV irradiation of $\sim$310 nm. Such a system enables us to cross-link the chains in semidilute solution to form a chemical gel in a controllable fashion.[33,34] It is important to note that such a UV-irradiation-induced sol−gel transition is different from the conventional UV-induced polymerization of vinyl monomers, i.e., there is no propagation. Each cross-linking reaction simultaneously involves only two very nearby coumarin groups so that the dimerization mostly occurs at the entangled points when the chains are overlapped in semidilute solution. This explains why the cross-linking results in a uniform and speckle-free gel. The dimerization stops as soon as the UV irradiation is removed. Such a system provides several advantages over a conventional chemical gelation; namely, homogeneous cross-linking, no byproduct, no initiator, and a controllable cross-linking rate.[3] Moreover, such a cross-linking is reversible under the UV irradiation of a wavelength shorter than $\sim$260 nm.[35−37] Practically, we have a well-defined chain length and a fixed polymer concentration. The UV reaction enables us to study the chain dynamics at each stage of the sol−gel transition, starting from a uniform semidilute solution without the complication of any frozen-in inhomogeneous component. In the present paper, we intend to further address the origin of the speckles and focus on the slow relaxation in the gel state as well as how it is related to the slow mode in semidilute solution.

Experimental Section

Sample Preparation. 7-Hydroxy-4-methyl coumarin and methacryloyl chloride (Acros) were used without further purification. Methyl methacrylate (MMA, Aldrich) was purified by vacuum distillation. AIBN (Aldrich) was purified by recrystallization from methanol. *N*,*N*-Dimethyl-formamide (DMF) was purified by vacuum distillation after drying with barium oxide. Other solvents and chemicals were used as received. The synthesis of photoreactive copolymer containing 4-methylcoumarin pendant groups involved two steps. The first step is to prepare 7-acryloyloxy-4-methylcoumarin (AMC). To a solution of 7-hydroxy-4-methyl coumarin (12.0 g, 68 mmol) in 192 mL of 0.5 N NaOH aqueous solution was added 150 mL chloroform and then cooled to 5 °C. Under vigorous stirring, methacryloyl chloride (7.1 g, 68 mmol) was injected into the mixture and the reaction was continued for 1 h. The white solid obtained after evaporating chloroform was recrystallized in acetone.[34,36] In the second step, AMC was copolymerized with methyl methacrylate (MMA) in DMF by using AIBN as initiator.[34,37] Freshly distilled MMA and AMC as well as AIBN solution were charged into a polymerization tube and [MMA]/[AMC]/[AIBN] = 9:1:0.0002. After three freeze−thaw cycles of degassing, the tube was sealed off under vacuum. The reaction was carried out at 60 °C for ∼40 h. The resultant copolymer P(MMA-*co*-AMC) was harvested in methanol and purified. The sample used contains 7.2 mol % of AMC and has a weighted-averaged molar mass (M_w) of 2.12×10^5 g/mol with a polydispersity index (M_w/M_n) of <1.5.[34]

Laser Light Scattering. A commercial spectrometer (ALV/DLS/SLS-5022F) equipped with a multi-τ digital time correlator (ALV5000) and a cylindrical 22 mW uniphase He−Ne laser ($\lambda_0 = 632$ nm) was used. The spectrometer has a high coherence factor of $\beta \sim 0.95$ because of a novel single-mode fiber optic coupled with an efficient avalanche-photodiode (APD). The starting semidilute solution used in this study was prepared by dissolving a proper amount of P(MMA-*co*-AMC) in chloroform. The clear solution was then filtered into a quartz LLS cell (10 mm in diameter) to remove dust by using PTFE 1.0 μm filter. The solution was sealed under nitrogen. The clarified solution was irradiated in a UV photoreactor equipped with 10 tubes of 310 nm lamps (total energy output of ∼150 W). The LLS study was conducted after different UV irradiation times.

In static LLS, the measurement time for each chosen sample position at a given scattering vector q [$\equiv 4\pi n \sin(\theta/2)/\lambda_0$] was 30 s, where θ, n, and λ_0 are the scattering angle, the solution refractive index, and the wavelength of the laser light in vacuum, respectively. In dynamic LLS, the measurement time of each time correlation function was in the range 30−60 min, depending on the signal-to-noise ratio. The first-order cumulant analysis of the initial decay of each measured baseline-normalized intensity−intensity time correlation function $g^{(2)}(q,\tau)$ [$\equiv \langle I(q,0)I(q,\tau)\rangle/\langle I(q,0)\rangle^2 - 1$] in the self-beating mode can result in an average characteristic decay time $\langle\tau_c\rangle$ or an average line width $\langle\Gamma\rangle$ ($\equiv 1/\langle\tau_c\rangle$) that is related to the apparent diffusion coefficient D_A [$\equiv \langle\Gamma\rangle/q^2$]. The details of the LLS instrumentation and theory can be found elsewhere.[38,39]

Data Analysis

Partial Heterodyne Method. For a nonergodic gel, the time-averaged scattered light intensity $\langle I\rangle_T$ comprises two contributions,[21]

$$\langle I\rangle_T = \langle I_s\rangle_T + \langle I_d\rangle_T \tag{1}$$

where $\langle I_s\rangle_T$ is related to frozen-in static component and varies with the sample position, but $\langle I_d\rangle_T$ is related to mobile dynamic component so that it is independent of the sample position. For each randomly chosen sample position, we can measure one $\langle I\rangle_T$ from static LLS as well as one $g^{(2)}(q,\tau)$ from dynamic LLS at a given scattering angle.[22,38] It is helpful to note that both $\langle I\rangle_T$ and $g^{(2)}(q,\tau)$ depend on the sample position. For an ergodic system, $\langle I_s\rangle_T = 0$ and $g^{(2)}(q,\tau)$ can be related to the normalized electric field-electric field time correlation function $|g^{(1)}(q,\tau)|$ ($\equiv [\langle E(q,0)E^*(q,\tau)\rangle/\langle E(q,0)E^*(q,0)\rangle]$) via the Siegert relation,[38]

$$g^{(2)}(q,\tau) \equiv \frac{\langle I(q,0)I(q,\tau)\rangle}{\langle I(q,0)\rangle^2} - 1 = \beta|g^{(1)}(q,\tau)|^2 \tag{2}$$

where $0 < \beta < 1$ is a constant related to the coherence of the detection optics. In a nonergodic gel, the frozen-in static components act as local oscillators so that $g^{(2)}(q,\tau)$ consists of both the homodyne and heterodyne terms. Equation 2 becomes[9,21−23]

$$g^{(2)}(q,\tau) = \beta\left\{\left(\frac{\langle I_d\rangle_T}{\langle I\rangle_T}\right)^2\left|g^{(1)}(q,\tau)\right|^2 + 2\left(\frac{\langle I_d\rangle_T}{\langle I\rangle_T}\right)\left[1 - \left(\frac{\langle I_d\rangle_T}{\langle I\rangle_T}\right)\right]\left|g^{(1)}(q,\tau)\right|\right\} \tag{3}$$

Equation 3 shows that the apparent coherent factor β_{app} {$\equiv \beta[2(\langle I_d\rangle_T/\langle I\rangle_T) - (\langle I_d\rangle_T/\langle I\rangle_T)^2]$}, i.e., the intercept of $g^{(2)}(q,\tau)$ at $\tau \rightarrow 0$, increases monotonically with $\langle I_d\rangle_T$ and its maximum value is β when $\langle I_d\rangle_T \rightarrow \langle I\rangle_T$. Note that $\langle I_s\rangle_T$ normally increases as the cross-linking proceeds so that $\langle I_d\rangle_T/\langle I\rangle_T$ decreases, resulting in a lower β_{app}, as observed in many previous studies of polymer gels.[9] As stated before, the initial slope of each measured "ln $g^{(2)}(q,\tau)$ vs τ" leads to an apparent line width Γ_A between 2Γ and Γ, depending on how strong $\langle I_d\rangle_T$ is, where Γ is the line width in a pure heterodyne measurement. It has been shown that Γ and $\langle I_d\rangle_T$ can be related to Γ_A and $\langle I\rangle_T$ as follows[21,25,26]

$$\frac{\langle I\rangle_T}{\Gamma_A} = \frac{2\langle I\rangle_T}{\Gamma} - \frac{\langle I_d\rangle_T}{\Gamma} \tag{4}$$

Experimentally, for each chosen sample position, one can measure one $\langle I\rangle_T$ from static LLS and calculate one Γ_A from $g^{(2)}(q,\tau)$ measured in dynamic LLS. Therefore, by randomly choosing a large number of different positions, we can obtain Γ and $\langle I_d\rangle_T$, respectively, from the slope and intercept of the plot "$\langle I\rangle_T/\Gamma_A$ versus $\langle I\rangle_T$" according to eq 4. It is very time-consuming to study the dynamics of a nonergodic gel in this way. The worst thing is that we can determine the initial decay only if the relaxation contains more than one process.

Intermediate Scattering Function Method. The normalized intermediate scattering function $f(q,\tau)$ provides an alternative way to analyze the dynamics of a nonergodic gel. It has been shown that $f(q,\tau)$ is related to $g^{(2)}(q,\tau)$ as follows:[21−24]

$$f(q,\tau) = 1 + \frac{\langle I\rangle_T}{\langle I\rangle_E}\left[\sqrt{1 - \left[\frac{g^{(2)}(q,0) - g^{(2)}(q,\tau)}{\beta}\right]} - 1\right] \tag{5}$$

At $\tau \rightarrow \infty$, $f(q,\tau) \rightarrow (\langle I\rangle_E - \langle I_d\rangle_T)/\langle I\rangle_E$. For an ergodic system, $\langle I\rangle_T = \langle I\rangle_E$ and $\langle I_s\rangle_T = 0$; namely, $\langle I_d\rangle_T = \langle I\rangle_E$ and $f(q,\infty) \rightarrow 0$. Therefore, $f(q,\infty)$ for a nonergodic system directly reflects the contribution of static frozen-in components. For each given scattering angle, we can measure the time-averaged scattering intensity from different sample positions to obtain $\langle I\rangle_E$, defined as $\sum_i \langle I\rangle_{T,i}/N$, where N is the total number of the sample positions measured. Therefore, $f(q,\tau)$ can be calculated from a single

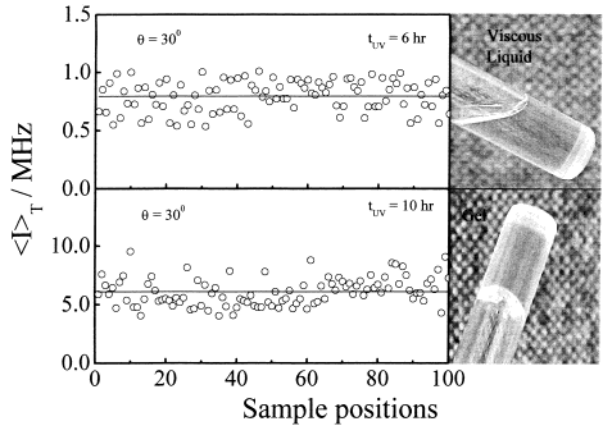

Figure 1. Sample position dependence of time-averaged scattering intensity $\langle I\rangle_T$, where each solid line represents an ensembly averaged scattering intensity $\langle I\rangle_E$ defined as $(\sum_i \langle I\rangle_{T,i})/N$ with N the total number of randomly chosen sample positions.

measurement of $g^{(2)}(q,\tau)$ and $\langle I\rangle_T$. It is important to note once more that for a given scattering angle, $\langle I_s\rangle_T$ and $\langle I\rangle_T$ as well as $g^{(2)}(q,0)$ and $g^{(2)}(q,\tau)$ depend on the sample position, but not $\langle I\rangle_E$, $\langle I_d\rangle_T$ and $f(q,\tau)$. Finally, note that in an ergodic system, $\langle I\rangle_T = \langle I\rangle_E$ and $g^{(2)}(q,0) \rightarrow \beta$ so that eq 5 goes back to eq 2 and $f(q,\tau) \rightarrow |g^{(1)}(q,\tau)|$.

Results and Discussion

Figure 1 shows that after 10 hr UV irradiation, a flowing semidilute solution changes into a macroscopically immobile chemical gel. The cross-linking density increases with an increasing irradiation time. The final cross-linking density is 2%, estimated from the change of AMC UV adsorption. The sample position was arbitrarily chosen by rotating and lifting the LLS cuvette. Each solid horizontal line indicates an ensembly averaged scattering intensity $\langle I\rangle_E$. The solution became viscous after 6 h UV irradiation but was still flowing when the cuvette was tilted. It is known that such a polymer solution must be ergodic. It is helpful to note that the scattering intensity after 6 h UV irradiation increases ~10 times in comparison with that from the initial semidilute solution (not shown). Further UV irradiation finally resulted in chemical gel, and the scattering intensity increased another ~10 times but still lacked obvious speckles, as shown in Figure 1. Note that the gelation threshold is located at $t_{UV} \cong 9$ h, confirmed by the flowing test.

Figure 1 is surprisingly different from previous observations on both chemical and physical gels in which $\langle I\rangle_T$ strongly depends on the sample position due to the so-called static frozen-in components.[25,26] Later, we will show that the increase of $\langle I\rangle_T$ can be related to the increase of the correlation between chains because of the interchain dimerization (cross-linking). The speckle-free pattern illustrates that the gel is uniform, suggesting that the cross-linked chains (clusters) are uniformly distributed inside and the size of the frozen-in clusters, if there were any, are much smaller than the linear dimension of the scattering volume (~200 μm). In other words, the scattering volume should contain a sufficient number of such clusters so that the invariant scattering intensity reflects an averaged result. In the present gel, the nature of the cross-linking ensures that no large void can be formed inside. We will come back to this point.

As for the study of gel dynamics, we first used the partial heterodyne method (eqs 3 and 4) to analyze the measured time correlation function by assuming that there exist some static frozen-in components. Figure 2 shows that the ratio of $\langle I\rangle_T/\Gamma_A$ is a linear function of $\langle I\rangle_T$, where the solid line shows the least-squares fitting on the basis of eq 4, in which the slope and

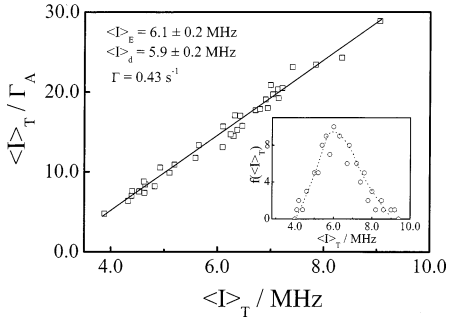

Figure 2. Typical plot of $\langle I\rangle_T/\Gamma_A$ versus time-average scattering intensity $\langle I\rangle_T$ for the gel formed after 10 h UV irradiation, where time-averaged scattering intensity from dynamic mobile components $\langle I_d\rangle_T$ and characteristic line width Γ are obtained from the intercept and the slope, respectively, on the basis of eq 4. The inset shows the frequency distribution of $\langle I\rangle_T$.

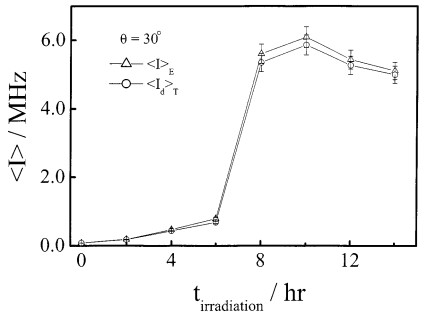

Figure 3. UV irradiation time dependence of ensembly averaged scattering intensity $\langle I\rangle_E$ and time-averaged scattering intensity from dynamic mobile components $\langle I_d\rangle_T$ during the sol−gel transition.

intercept lead to Γ and $\langle I_d\rangle_T$, respectively. Therefore, we were able to obtain the q-dependence of $\langle I\rangle_E$, $\langle I_d\rangle_T$, and Γ at each stage of the sol−gel transition. It is helpful to note that for a normal gelation process it is rather difficult to obtain such q-dependence because of the progress of the reaction during the measurement. Figure 2 shows that the difference between $\langle I\rangle_E$ and $\langle I_d\rangle$ is so small that $\langle I\rangle_E \approx \langle I_d\rangle_T$ if we consider all experimental uncertainties. This can be attributed to the random fluctuation of $\langle I\rangle_T$ around $\langle I\rangle_E$ (Figure 1). The inset shows that $\langle I\rangle_T$ roughly follows a Gaussian distribution, a characteristic signature of ergodicity. It is important to note that for conventional polymer gels, the frequency distribution $f(\langle I\rangle_T)$ decreases monotonically as $\langle I\rangle_T$ increases and the variation of $\langle I\rangle_T$ is often over $\sim 10^2$ times due to large frozen-in components.[9,25] It is also important to note that Γ obtained here is several orders smaller (i.e., the relaxation is much slower) than those previously obtained in conventional polymer gels.[16] Later, we will show that Γ obtained in Figure 2 is related to thermally agitated slow density fluctuation, not the fast diffusion of subchains (blobs) between two cross-linking points.

Figure 3 shows that for a given q, the variation of both $\langle I\rangle_E$ and $\langle I_d\rangle_T$ can be divided into three different stages during the sol−gel transition. In the first stage ($t_{UV} < 6$ h), $\langle I\rangle_E$ equals $\langle I_d\rangle_T$ because the solution is ergodic. The gradual increase of $\langle I\rangle_E$ (or $\langle I_d\rangle_T$) is expected due to the cross-linking of individual copolymer chains. In the second stage (6 h $< t_{UV} <$ 8 h), the rapid increase of $\langle I\rangle_E$ (and $\langle I_d\rangle_T$) signals the formation of more branched chains (clusters). The system reaches the gelation threshold at ~9 h, which was also confirmed by the flowing test. Such an abrupt increase of the scattered light intensity is often used to define the gelation threshold.[40] The only difference here is that the resultant gel lacks large obvious speckles. At the final stage, further cross-linking slightly reduces both $\langle I\rangle_E$ and $\langle I_d\rangle_T$, revealing that the density fluctuation in space is

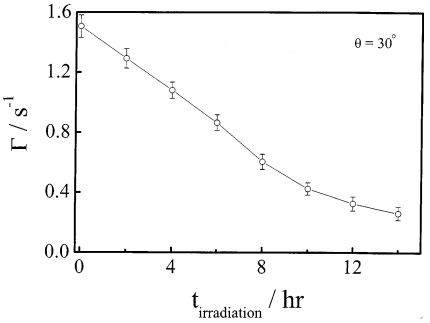

Figure 4. UV irradiation time dependence of characteristic line width Γ during the sol−gel transition, where Γ was obtained based on eq 4, as shown in Figure 2.

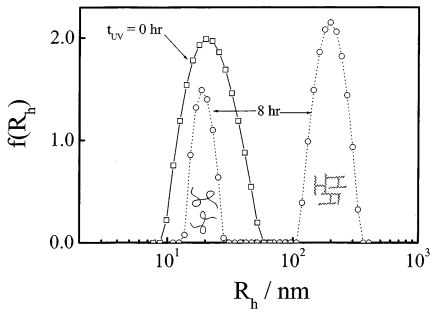

Figure 5. Hydrodynamic radius distributions $f(R_h)$ of photocrosslinkable [P(MMA-*co*-AMC)] chains in dilute chloroform solution before and after 8 h UV irradiation, where polymer concentration C is only 2.0×10^{-4} g/mL, which is ∼10 times less than the overlap concentration C^*.

slightly suppressed. This can be visualized as individual chains are attached to the gel network and the contrast between denser and sparser parts of the density fluctuation gradually decreases. It is important to note that during the entire sol-to-gel process, $\langle I \rangle_E \cong \langle I_d \rangle_T$ if we consider all experimental uncertainties.

Figure 4 shows that the line width (Γ) obtained in the partial heterodyne analysis of $g^{(2)}(\tau)$ continuously decreases as the cross-linking proceeds, which is different from previous results. For example, Shibayama et al.[16] showed that Γ increased with the cross-linking density and attributed it to the decrease of the dynamic correlation length ($\xi_{dynamic}$) or the mesh size. In the present case, the photodimerization of two coumarin groups interconnects long linear entangled chains into branched chains and finally an "infinite" gel network. Once more, it is helpful to note that the nature of the dimerization determines that it can occur only between two very nearby coumarin groups. Therefore, the cross-linking mostly occurs at the entangled points. In this way, the cross-linking should induce no big change in the average length of the subchain (blobs) between two entangled points in semidilute solution. Γ is several orders slower than previously reported values.[9,16] Therefore, its related relaxation cannot be attributed to the fast motions of the subchains (blobs) between two cross-linking points. To have a more clear picture of the size of the polymer clusters (branched chains) formed during the sol−gel transition, a small amount of the sample was drawn, diluted, and characterized by dynamic LLS before the system reaches the gelation point.

As expected, Figure 5 shows that $f(R_h)$ initially has only one expected peak related to individual linear copolymer chains in dilute solution, but the cross-linking results in a bimodal distribution. The second peak located at ∼200 nm is related to large clusters formed after 8 h UV irradiation. Note that the gelation threshold is ∼9 h UV irradiation. The size distribution of the resultant polymer clusters is surprisingly narrow, suggesting that the cross-linking is predominantly controlled by a

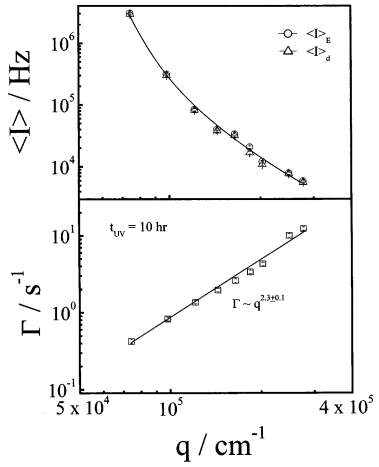

Figure 6. Scattering vector dependence of ensembly averaged scattering intensity $\langle I \rangle_E$, time-averaged scattering intensity from dynamic mobile components $\langle I_d \rangle_T$ and characteristic line width Γ of the gel formed after 10 h UV irradiation.

diffusion-limited process.[41] Since the concentration ($C = 8.0 \times 10^{-2}$ g/mL) used in the sol−gel transition is much higher than the overlap concentration ($C^* \sim 1.8 \times 10^{-3}$ g/mL), the dimerization (cross-linking) should mostly occur between different chains at the entangled points, leading to randomly branched clusters, schematically shown in Figure 5. It is important to note that the clusters are much smaller than the linear dimension of the scattering volume (∼200 μm). The cross-linking in the present study is extremely slow, and the nature of the dimerization avoids the formation of large voids inside. As discussed before, to prepare a more homogeneous gel, one has to make the growing rate of the polymer clusters much slower than their diffusion so that large polymer clusters have a sufficient time to relax to their equilibrium positions before they are stuck in space to form large voids.

Figure 6 shows that in the gel state both $\langle I \rangle_E$ and $\langle I_d \rangle_T$ dramatically decrease with an increasing scattering vector q, where the scattering volume has already been corrected by a factor of $\sin(\theta)$. In LLS, $1/q$ is the observation length and a higher q means that the light probes a smaller dimension in real space. The length of $1/q$ used here ranges from 35 to 150 nm. The fact that $\langle I \rangle_E \approx \langle I_d \rangle_T$ over the entire q range further indicates that such a gel is homogeneous and the excursion of the density fluctuation is over ∼100 nm within the delay time window of a few seconds used in dynamic LLS. On the other hand, the strong angular dependence reveals that the dimension of the density fluctuation in real space must extend over ∼100 nm.[23] Figure 6 also shows that Γ is scaled to q as $\Gamma \propto q^{2.3\pm0.1}$, indicating that the relaxation obtained in the partial heterodyne analysis is not purely diffusive. Unfortunately, some of previous studies obtained Γ only from one scattering angle (90°), and the related relaxation was automatically attributed to be the cooperative diffusion.[9,10,25] Later, in the intermediate scattering function analysis, such a nondiffusive nature will become more clear.

We previously showed that in the semidilute solutions with different concentrations there always exist a fast and a slow relaxation mode. The fast mode ($\Gamma_f \sim 10^4$ s^{-1} i.e., $D_c = \Gamma_f/q^2 \sim 10^{-6}$ cm^2/s) is diffusive, while the slow fluctuation ($\Gamma_s \sim 10^0$ s^{-1}) measures internal motions of large transient clusters (density fluctuation) with a finite long lifetime.[34] Note that Γ in Figure 6 is in the same order as Γ_s measured in the semidilute solutions, much larger than Γ_f. This forces us to think about the nature of Γ obtained in the partial heterodyne analysis based on eqs 3 and 4. As discussed before, Γ_s in the past was sometimes

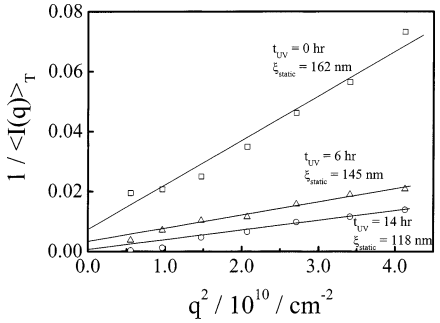

Figure 7. Typical Ornstein−Zernike plots of $1/\langle I(q)\rangle_T$ vs q^2, where $\langle I(q)\rangle_T$ is time-averaged scattering intensity at scattering vector q. The ratio of the slope to the intercept leads to static correlation length (ξ) on basis of eq 6.

wrongly attributed to the repetition of individual chains in the matrix (tube) made of other chains because dynamic LLS is not able to probe the diffusion of individual chains in semidilute solution, except that a small number of chains (probes) are marked with a large refractive index difference. Note that in the past Γ_s was also attributed to the diffusion of the associated chains, but no explanation was given why homopolymer chains could associate with each other in good solvent.[42] Also noted that there has been a suggestion that Γ_s is related to the density fluctuation,[43] but no explanation was given to the variation of why the scaling exponent α_s in $\Gamma_s \sim q^{\alpha_s}$.

When discussing the density fluctuation, we should note that there are three different parameters related to such a fluctuation; namely, its dimension (size), its amplitude (the contrast between denser and sparser parts), and its frequency. They are respectively related to the static correlation length (ξ_{static}), the scattering intensity ($\langle I\rangle_T$), and the line width (Γ) of the relaxation. It has been known that ξ_{static} inside a semidilute solution or a gel network can be related to the scattering light intensity ($I(q)$) and the scattering vector (q) by the Ornstein−Zernike equation:[44,45]

$$I(q) = \frac{I(q \to 0)}{1 + q^2 \xi^2_{static}} \tag{6}$$

Figure 7 shows typical Ornstein−Zernike plots of $1/I(q)$ versus q^2, where ξ_{static} was calculated from the slope-to-intercept ratio. It is clear that the density fluctuation has a length scale over ~100 nm. The decrease of ξ_{static} is expected because the cross-linking increases the solution viscosity and modulus. It is important to note that at the same time, the scattering intensity increases $\sim 10^2$ times as the cross-linking proceeds (Figure 1). This is because the cross-linking makes the fluctuation of different chains more correlated. Keep this in mind because we will need it later to discuss the change of the scaling exponent α_s between Γ_s and q.

Figure 8a shows that just like in the semidilute solution ($t_{UV} = 0$ h), $g^{(2)}(q,\tau)$ of partially cross-linked chains at $t_{UV} \sim 6$ h also contains two relaxation modes. Previous studies of other semidilute solutions have already confirmed that the fast relaxation corresponds to the cooperative diffusion of the subchains between two entangled points, well described by the "blob" or the scaling theory. There are also indications that the slow relaxation is related to internal motions of entangled chains.[46−48] Note that the extent of each relaxation (the height of each step) in Figure 8 represents its intensity contribution. It is clear in Figure 8a that as the cross-linking proceeds the slow relaxation becomes even slower and contributes more and more, while the fast relaxation apparently disappears. However, Figure 8b reveals that even in the fully developed gel state, the fast

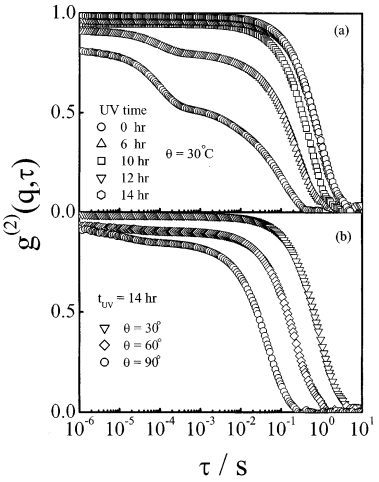

Figure 8. (a) UV irradiation time dependence of intensity−intensity time correlation function $g^{(2)}(q,\tau)$ during the sol−gel transition and (b) scattering vector dependence of $g^{(2)}(q,\tau)$ of the gel formed after 14 h UV irradiation.

mode still exists at a higher q, i.e., a smaller observation length ($1/q$). This point has been overlooked in the past.

It is important to note that after 12 h UV irradiation, the slow down of the relaxation ceases and there is no further change in the slow dynamics. Unlike other sol−gel transitions,[7−9,16] here we observed no critical slow down and no scaling between $g^{(2)}(q,\tau)$ and τ over the whole delay time window, i.e., the plot of "log $g^{(2)}(q,\tau)$ vs log τ" is not a straight line. This is understandable because the photoreactive coumarin groups attached on the polymer chain can only fluctuate around their equilibrium positions in viscous semidilute solution, so that they have less or even no chance to further interconnect with each other after individual chains become part of the gel network. In contrast, in the formation of conventional chemical gels, small cross-linking agents and monomers can continuously diffuse and react inside the swollen gel network, even after passing the gelation threshold.

Another surprising observation is that the apparent coherent factor (β_{app}), the intercept of $g^{(2)}(q,\tau)$ at $\tau \to 0$, increases during the sol−gel transition. This is opposite to the decrease of β_{app} observed in previous studies, e.g., by Martin et al.[8] in the gelation of TMSO, by Shibayama et al.[9,49] in bulk cross-linking polymerization of *N*-isopropylacrylamide (NIPA), and by Fang et al.[24] in the formation of poly(acrylamide) gels. The decrease of β_{app} was attributed to the formation of large frozen-in static components (large voids) because the light scattered from them raises the baseline.[23] A reasonable explanation of the increase of β_{app} in Figure 8 is as follows. The scattered light intensity comes from solvent (I_s), chain segments (I_{blobs}), and large polymer "clusters" ($I_{cluster}$), i.e., $I_{solution} = I_s + I_{blobs} + I_{cluster}$. Let us not consider the nature of the clusters at this moment. Here, I_s normally contributes so little that it can be neglected. Therefore, the intensity−intensity time correlation function $G^2(q,\tau)$ becomes $\langle[I_{blobs}(q,0) + I_{cluster}(q,0)][I_{blobs}(q,\tau) + I_{cluster}(q,\tau)]\rangle$. The relaxation of the blobs is much faster than that of larger "clusters", evidenced in Figure 8. Thus, $g^{(2)}(q,\tau)$ can be approximated as[50]

$$g^{(2)}(q,\tau) \approx \beta\left[\frac{I_{cluster}}{I_{solution}}\left|g^{(1)}{}_{cluster}(q,\tau)\right|\right]^2 \tag{7}$$

where for the simplicity of the discussion we did not consider the cross-correlation term between the blobs and large clusters. In comparison with eq 2, it is clear that the observed intercept is an apparent coherent factor β_{app}. Initially, I_{blobs} is comparable

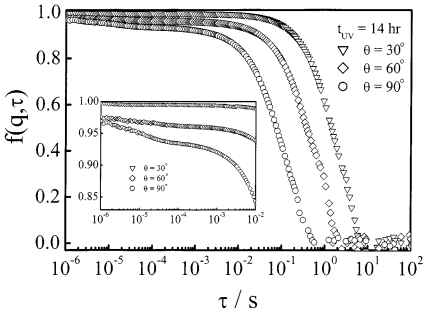

Figure 9. Scattering vector dependence of normalized intermediate scattering function $f(q,\tau)$ of the gel formed after 14 h UV irradiation. The inset shows an enlargement of the initial decay of each $f(q,\tau)$.

to $I_{cluster}$ so that β_{app} is only a fraction of β. As the cross-linking proceeds, $\langle I\rangle_T$ increases $\sim 10^2$ times, mainly due to the increase of $I_{cluster}$ (as will be shown later) so that $I_{cluster}/I_{solution} \rightarrow 1$. This is why β_{app} approaches β ($\sim$0.95) as the cross-linking proceeds. Following this argument, we can explain why β_{app} at a smaller scattering angle is higher (Figure 8b). This is because at a lower scattering angle ($1/q$ is larger), one large object scatteres much more light than one smaller object so that the relative contribution of $I_{cluster}$ to $I_{solution}$ is higher. Moreover, Figure 8 shows that even for the fully developed gel, $G^{(2)}(q,\tau)$ still fully relaxes to zero within the delay time window of a few seconds. It has to be stated once more that such a complete relaxation is not due to the improper normalization as mistakenly done in previous studies, because here β_{app} increases during the sol−gel transition. Such a complete relaxation can be better viewed in terms of the normalized intermediate scattering function $f(q,\tau)$ defined on the basis of eq 5.

Figure 9 shows that $f(q,\tau)$ at each scattering angle can fully relax to zero, similar to an ergodic polymer solution, but the relaxation is much slower. This further shows that the complete relaxation of $g^{(2)}(q,\tau)$ to zero in Figure 8 is not due to an improper baseline normalization. To our knowledge, this is the first observation for a chemical gel that $f(q,\tau)$ can completely decay to zero. In previous studies of different chemical and physical gels, $f(q,\tau)$ only decay to a nonzero plateau, reflecting the static frozen-in components inside.[23,27,51] Note that in the present gel, the polymer chains are chemically cross-linked and fixed in a three-dimensional macroscopically immobile network, just as any other chemical gels. The only difference is that the cross-linking in the present gelling system introduces no large void inside. The full relaxation of $f(q,\tau)$ in Figure 9 reveals that the excursion of the cross-linked chains inside the gel network is over the length scale of $1/q$ ($\sim$100 nm). This further convinces us that the static frozen-in components inside polymer gels are large voids, not the cross-linked chains (clusters). It is not difficult to visualize that in conventional gels large voids cannot relax, but the cross-linked chains surround them can still relax over a length of $1/q \sim 100$ nm.

The inset in Figure 9 is an enlargement of the initial decay, which clearly shows that there still exists a fast relaxation mode even in the gel state, especially when the observation length scale ($1/q$) is smaller. The relatively larger contribution of the fast relaxation at a smaller observation length further indicates that the fast mode is related to some localized motions of the subchains. To qualitatively extract the information related to these two modes, we combined an exponential decay for the fast mode and a stretched exponential decay for the slow mode, which is normally used for semidilute solution, as follows.[6−9,51−53]

$$f(q,\tau) = A_f \exp\left(-\frac{\tau}{\langle\tau_c\rangle_f}\right) + A_s \exp\left[-\left(\frac{\tau}{\langle\tau_c\rangle_s}\right)^b\right] \qquad (8)$$

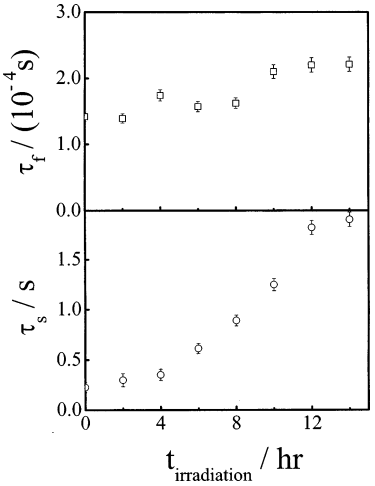

Figure 10. UV irradiation time dependence of fast and slow characteristic decay times ($\langle\tau_c\rangle_f$ and $\langle\tau_c\rangle_s$) during the sol−gel transition, where $\langle\tau_c\rangle_f$ and $\langle\tau_c\rangle_s$ were calculated on the basis of eq 8.

where A and $\langle\tau_c\rangle$ are the intensity weighting and characteristic decay time, respectively; subscripts "s" and "f" denote the fast and slow modes, respectively; and $0 < b < 1$, a constant related to the distribution width of the slow relaxation mode. Note that $A_f + A_s = 1$.

Figure 10 shows that during the sol−gel transition, the characteristic decay time $\langle\tau_c\rangle_f$ of the fast mode only slightly increases, while for the slow mode, $\langle\tau_c\rangle_s$ starts to increase after 4 h UV irradiation and levels off at $t_{UV} \sim 12$ h, indicating that the relaxation becomes slower and slower as the cross-linking proceeds. It is helpful to note that the characteristic relaxation time is proportional to the friction coefficient (ζ) but reciprocally proportional to the elastic and shear modulus.[54] As expected, both the modulus and ζ increase as the cross-linking proceeds. The slow-down of the slow relaxation could be related to the increase of the dimension of the density fluctuation. However, Figure 7 shows that ξ_{static} decreases as the cross-linking proceeds. Therefore, the increase of $\langle\tau_c\rangle_s$ could only be attributed to the viscoelastic effect, presumably that ζ effects $\langle\tau_c\rangle_s$ more than the modulus. Note that the increase of $\langle\tau_c\rangle_s$ is only $\sim$6 times, which rejects the possibility that the slow relaxation is related to the diffusion of the associated polymer chains. If this was the case, $\langle\tau_c\rangle_s$ would increase much more as the cross-linking proceeds because the diffusion of branched chains (clusters) is extremely slow inside a gel network. On the other hand, the lessened effect of the cross-linking on $\langle\tau_c\rangle_f$ is reasonable because the fast relaxation is related to the local motions of the subchains ("blobs") between two entangled points. The cross-linking should not largely change the local viscosity around the subchains or the average length of the subchains because the dimerization mostly occurs at the entangled points. Otherwise, $\langle\tau_c\rangle_f$ should decrease as in conventional chemical gels. The slight increase of $\langle\tau_c\rangle_f$ is also understandable because the cross-linking slightly hinders the motions of the subchains in comparison with that in the semidilute solution in which the chains are only entangled.

Figure 11 shows that in the semidilute solution Γ_f ($=1/\langle\tau_c\rangle_f$) $\propto q^{\alpha_f}$ and Γ_s ($=1/\langle\tau_c\rangle_s$) $\propto q^{\alpha_s}$ with $\alpha_f = 2.0 \pm 0.1$ and $\alpha_s = 3.0 \pm 0.1$, while in the gel state α_f increases to 2.4 ± 0.1 but α_s decreases to 2.3 ± 0.1. It is well known from the LLS theory that for a given scattering object with a size R, the scaling exponent between Γ and q increases from 2 to 3 when $1/q \ll R$ changes to $1/q \gg R$.[38,39] The increase of α_f indicates that the cross-linking makes the motions of different blobs becomes more correlated. The decrease of α_s is related to the change of the dimension of the density fluctuation. As shown in Figure

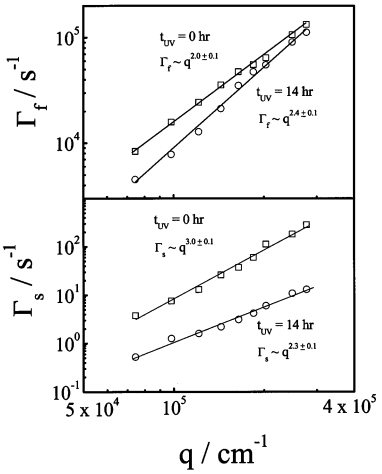

Figure 11. Scattering vector dependence of fast and slow characteristic decay times ($\langle\tau_c\rangle_f$ and $\langle\tau_c\rangle_f$) of initial semidilute solution and resultant chemical gel, where $\langle\tau_c\rangle_f$ and $\langle\tau_c\rangle_s$ were calculated on the basis of eq 8.

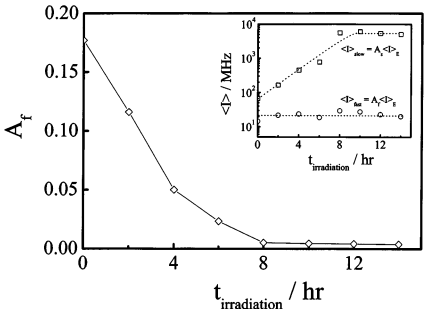

Figure 12. UV irradiation time dependence of relative intensity contribution of fast relaxation mode [$A_f = \langle I\rangle_{fast}/(\langle I\rangle_{fast} + \langle I\rangle_{slow})$] during the sol−gel transition. The inset shows UV irradiation time dependence of the scattering intensities related to the fast and slow modes $\langle I\rangle_{fast}$ and $\langle I\rangle_T A_s$.

7, in the semidilute solution $\xi_{static} > 1/q$ so that the light probes the internal motions of large density fluctuation and $\alpha_s \approx 3.0 \pm 0.1$, while in the gel state $\xi_{static} \sim 1/q$ so that the light detects only part of internal motions, similar to the study of long polymer chains or large microgels when $1/q$ is comparable to the size of the chain.[55,56] This is why α_s decreases from 3.0 to 2.3. The nature of the fast and slow modes can be better viewed in terms of the variation of their related scattering intensities during the sol−gel transition.

Figure 12 shows that the relative intensity contribution of the fast relaxation mode [$A_f = \langle I\rangle_{fast}/(\langle I\rangle_{fast} + \langle I\rangle_{slow})$] decreases as the cross-linking proceeds. Note that at the same time the overall time-averaged scattering intensity ($\langle I\rangle_T$) increases $\sim 10^2$ times during the sol−gel transition. The inset of Figure 12 shows that the absolute scattering intensity related to the fast mode ($\langle I\rangle_{fast} = \langle I\rangle_T A_f$) actually remains a constant. Unfortunately, previously reported studies never realized such important information, which can be easily obtained from a combination of static and dynamic LLS. The constant $\langle I\rangle_{fast}$ and the near constant $\langle\tau_c\rangle_f$ directly reveal that the cross-linking indeed mostly occurs at the entangled points so that there is no significant change in the average length of the subchains (blobs). Otherwise, both $\langle I\rangle_{fast}$ and $\langle\tau_c\rangle_f$ would change as the cross-linking proceeds. On the other hand, the inset clearly shows that the cross-linking greatly increases the scattering intensity related to the slow relaxation ($\langle I\rangle_{slow}$). A combination of Figures 7 and 12 shows that the increase of $\langle I\rangle_{slow}$ is not due to the increase of ξ_{static}. The increase of $\langle I\rangle_{slow}$ further excludes any possibility of attributing the slow relaxation to the diffusion of individual chains or clusters inside the gel network. If that was the case,

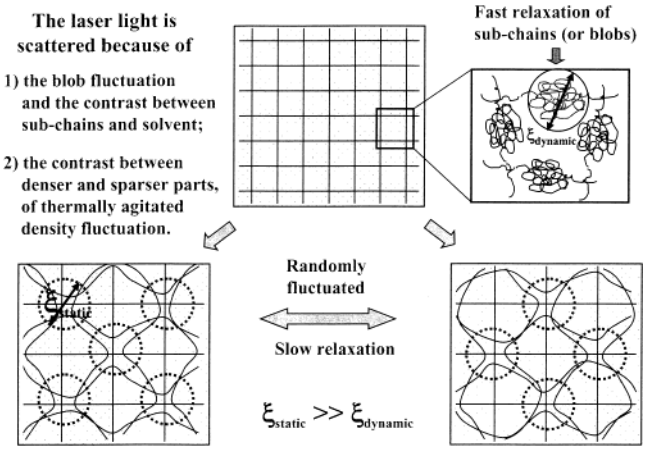

Figure 13. Schematic of fast and slow relaxation modes of a uniform gel network swollen in good solvent.

the scattering intensity related to the slow relaxation would decrease because the number of individual chains or clusters in the gel network should decrease as the cross-linking proceeds. As discussed before, the increase of $\langle I\rangle_{slow}$ is because the cross-linking makes the scattered light from different blobs more correlated. The level-off of $\langle I\rangle_{slow}$ indicates that most of the coumarin groups at the entangled points are reacted, and further UV irradiation has less effect on the gel network.

Figure 13 schematically summarizes the above discussion about the fast and slow modes. Let us start with a uniform gel network. Such an ideal gel network also scatters the light because of the fluctuation of the subchains (blobs) around their equilibrium positions and the refractive index contrast between polymer and solvent. If the blobs are sufficient long, the thermally agitated random motions (relaxation) should be diffusive with a dynamic correlation length ($\xi_{dynamic}$) of $\sim$10 nm. The cross-linking makes the motions of different blobs more correlated to each other so that α_f increases. On the other hand, the thermal agitation also induces a large, but slow density fluctuation of the gel network over a length scale of $\sim$100 nm so that parts of the gel network become denser, as marked with the dash cycles in Figure 13. The refractive index contrast between denser and sparser parts leads to an additional scattering. The thermally agitated density fluctuation should be random, behaving just like the slow diffusion of large "clusters" randomly from one place to another. The scattering exponent α_s ranges between 2 and 3, depending on whether the range of $1/q$ is much larger or smaller than the dimension of the density fluctuation. The difference between a semidilute solution and a gel network is that the cross-linking hinders the density fluctuation, reduces its dimension, and increases its amplitude (the contrast between denser and sparser parts). As expected, for a gel network with a much higher cross-linking density, the motions of the blobs are suppressed and the dimension of the density fluctuation becomes much smaller than $1/q$. This might explain why only one q^2-dependent relaxation was observed in some previous studies of highly cross-linked chemical gels. It should be noted that in the study of polystyrene semidilute solution, Strobl et al.[57] did find that the slow relaxation is diffusive when they used an extremely large range of $1/q$. It is helpful to note that the density fluctuation is also influenced by the chain length and concentration. A qualitative prediction of different effects is much needed.

Conclusion

The incorporation of the photocrosslinkabe group 7-acryloyloxy-4-methyl-coumarin (AMC) into poly(methyl methacrylate)

(PMMA) chain backbone enables us to convert a semidilute solution to a chemical gel in a controllable fashion. Such a resultant gel is homogeneous and speckle-free; namely, the time-averaged scattering intensity ($\langle I\rangle_T$) equals the ensembly averaged scattering intensity ($\langle I\rangle_E$) over different sample positions. The lack of obvious speckles simplifies the study of gel dynamics. Our results showed that there always exist two relaxation modes during the sol−gel transition; even the fast mode sometimes apparently disappears at smaller scattering angles. These two modes can be traced back to the two corresponding modes in semidilute solution; namely, the fast diffusion of the subchains (blobs) between two entangled points and the slow thermally agitated density fluctuation. In the present system, the characteristic decay time ($\langle\tau_c\rangle_f \sim 10^{-4}$ s) of the fast relaxation is much faster than that of the slow relaxation ($\langle\tau_c\rangle_s \sim 10^0$ s). The complete relaxation of the normalized intermediate scattering function $f(q,\tau)$, a direct measurement of the static frozen-in components, reveals that the excursion of the cross-linked chains on the gel network is over the length scale of $1/q \sim 150$ nm during the delay time window of a few seconds used in dynamic LLS. It further indicates that the static frozen-in components inside conventional gels are large voids formed during the sol−gel transition. Therefore, the speckles of polymer gel is not intrinsic. Using such a concept, we can satisfactorily explain the effects of the amount of cross-linking agents, the swelling extent, the reaction rate, and the solvent quality on the inhomogeneity as well as on the scattering intensity. During the sol−gel transition, $\langle\tau_c\rangle_f$ and its related scattering intensity $\langle I\rangle_{fast}$ remain constants, revealing that the cross-linking mostly occurs at the entangled points and has no effect on the length of the subchains (blobs). On the other hand, the cross-linking reduces the dimension of the density fluctuation (ξ_{static} decreases), slows down the density fluctuation ($\langle\tau_c\rangle_s$ becomes longer), and increases the contrast between denser and sparser parts of the density fluctuation ($\langle I\rangle_{slow}$ increases). In comparison with the chain dynamics in semidilute solution, the cross-linking, as expected, makes the motions of different "blobs" less independent so that the scaling exponent (α_f) in $1/\langle\tau_c\rangle_f \sim q^{\alpha_f}$ increases, and at the same time, the relative LLS observation length ($1/q$) decreases so that α_s decreases from 3.0 to 2.3.

Acknowledgment. The financial support of the Hong Kong Special Administration Region Earmarked Grants (CUHK4025/02P, 2160181), the Special Funds for Major State Basic Research Projects (G1999064800), and the 2002/03 NNSFC Project (20274045) is gratefully acknowledged.

References and Notes

(1) Rossi, D.; Kajiwara, K.; Osada, Y.; Yamauchi, A., Eds.; *Polymer Gels*; Plenum: New York, 1991.
(2) Brinker, C. J.; Scherer, G. W. In *Sol−Gel Science*; Academic Press: San Diego, 1990.
(3) Osada, Y.; Kajiwara, K., Eds.; *Gels Handbook The Fundamentals*; Academic Press: San Diego, London, 2001; Vol 1.
(4) Norisuye, T.; Masui, N.; Kida, Y.; Ikuta, D.; Kokufuta, E.; Ito, S.; Panyukov, S.; Shibayama, M. *Polymer* **2002**, *43*, 5289.
(5) Brown, W., Ed. *Dynamic Light Scattering, the Methods and Application*; Clarendon: Oxford, 1993.
(6) Adam, M.; Delsanti, M.; Munch, J. P.; Durand, D. *Phys. Rev. Lett.* **1988**, *61*, 706.
(7) Martin, J. E.; Wilcoxon, J. *Phys. Rev. Lett.* **1988**, *61*, 373.
(8) Martin, J. E.; Wilcoxon, J.; Odinek, J. *Phys. Rev. A* **1991**, *43*, 858.
(9) Shibayama, M.; Norisuye, T. *Bull. Chem. Soc. Jpn*. **2002**, *75*, 641 and the references therein.
(10) Tanaka, T.; Hocker, L. O.; Benedek, G. B. *J. Chem. Phys*. **1973**, *59*, 5151.
(11) Munch, J. P.; Ankrim, M.; Hild, G.; Candau, S. *J. Phys. Lett. (Fr)* **1983**, *44*, L-37.
(12) Pusey, P. N.; van Megen, W. *Physica A* **1989**, *157*, 705.
(13) Panyukov, S.; Rabin, Y. *Macromolecules* **1996**, *29*, 7690.
(14) Pusey, P. N. *Macromol. Symp*. **1994**, *79*, 17.
(15) Wu, C.; Zuo, J.; Chu, B. *Macromoleucles* **1989**, *22*, 633. Wu, C.; Zuo, J.; Chu, B. *Macromoleucles* **1989**, *22*, 838.
(16) Shibayama, M. *Macromol. Chem. Phys.* **1998**, *199*, 1 and the references therein.
(17) Panyukov, S.; Rabin, Y. *Phys. Rep.* **1996**, *269*, 1.
(18) Mallam, S.; Horkay, F.; Hecht, A. M.; Geissler, E.; Renie, A. R. *Macromolecules* **1991**, *24*, 543.
(19) Horkay, F.; Hecht, A. M.; Mallam, S.; Geissler, E.; Renie, A. R. *Macromolecules* **1991**, *24*, 2896.
(20) Shibayama, M.; Tanaka, T.; Han, C. C. *J. Chem. Phys.* **1992**, *97*, 6892.
(21) Rouf, C.; Bastide, J.; Pujol, J. M.; Schosseler, F.; Munch, J. P. *Phys. Rev. Lett.* **1994**, *73*, 830.
(22) Joosten, J. G. H.; Gelade, E.; Pusey, P. N. *Phys. Rev. A* **1990**, *42*, 2161.
(23) Joosten, J. G. H.; Mccarthy, J. L.; Pusey, P. N. *Macromolecules* **1991**, *24*, 6690.
(24) Fang, L.; Brown, W. *Macromolecules* **1992**, *25*, 6897.
(25) Shibayama, M.; Norisuye, T.; Nomura, S. *Macromolecules* **1996**, *29*, 8746.
(26) Ikkai, F.; Shibayama, M. *Phys. Rev. Lett.* **1999**, *82*, 4946.
(27) Moussaid, A.; Slot, H. J. M.; Joosten, J. G. H. *Int. J. Polym. Anal. Charact.* **1995**, *2*, 43.
(28) Ikkai, F.; Shibayama, M. *Phys. Rev. E. Rapid Commun.* **1997**, *56*, R51.
(29) Shibayama, M.; Ikkai, F.; Shiwa, Y.; Rabin, Y. *J. Chem. Phys.* **1997**, *107*, 5227.
(30) Moussaid, A.; Munch, J. P.; Schosseler, F.; Candau, S. J. *J. Phys. II (Les Ulis, Fr.)* **1991**, *1*, 637.
(31) Zhao, Y.; Zhang, G. Z.; Wu, C. *Macromolecules* **2001**, *34*, 7804.
(32) Krall, A. H.; Huang, Z.; Weitz, D. A. *Physica A* **1997**, *235*, 19.
(33) Kuznetsova, N. A.; Kaliya, O. L. *Russ. Chem. Rev*. **1992**, *61*, 683.
(34) Ngai, T.; Wu, C. *Macromolecules* **2003**, *36*, 848.
(35) Li, W. J.; Lynah, V.; Thompson, H.; Fox, M. A. *J. Am. Chem. Soc*. **1997**, *119*, 7211.
(36) Chen, Y.; Geh, J.-L. *Polymer* **1996**, *37*, 4481.
(37) Chen, Y.; Wu, J.-D. *J. Polym. Sci., Polym. Chem. Edu*. **1994**, *32*, 1867.
(38) Berne, B. J.; Pecora, R. *Dynamic Light Scattering*; Plenum Press: New York, 1976.
(39) Chu, B. *Laser Light Scattering*, 2nd ed.; Academic Press: New York, 1991.
(40) Norisuye, T.; Shibayama, M.; Nomura, S. *Polymer* **1998**, *39*, 2769.
(41) Carpineti, M.; Giglio, M. *Phys. Rev. Lett.* **1993**, *70*, 3828.
(42) Nyden, M.; Soderman, O. *Macromolecules* **2000**, *33*, 1473.
(43) Brown, W.; Nicolai, T. *Colloid Polym. Sci.* **1990**, *268*, 977.
(44) Bueche, F. *J. Colloid Interface* **1970**, *33*, 61.
(45) Soni, V. K.; Stein, R. S. *Macromolecules* **1990**, *23*, 61.
(46) Konak, C.; Helmstedt, M.; Bansil, R. *Macromolecules* **1997**, *30*, 4342.
(47) Nemoto, N.; Koike, A.; Osaki, K. *Macromolecules* **1996**, *29*, 1445.
(48) Nystrom, B.; Thuresson, K.; Lindman, B. *Langmuir* **1995**, *11*, 1994.
(49) Takeda, M.; Norisuye, T.; Shibayama, M. *Macromolecules* **2000**, *33*, 2909.
(50) Wu, C.; Chu, B. In *Experimental Methods in Polymer Science: Modern Methods in Polymer Research and Technology*; Tanaka, T., Ed.; Academic Press: San Diego, 2000; pp 10−20.
(51) Rodd, A. B.; Dunstan, D. E.; Boger, D. V.; Schmidt, J.; Burchard, W. *Macromolecules* **2001**, *34*, 3339.
(52) Krall, A. H.; Weitz, D. A. *Phys. Rev. Lett.* **1998**, *80*, 778.
(53) Fuchs, T.; Richtering, W.; Burchard, W.; Kajiwara, K.; Kitamura, S. *Polym. Gels Networks* **1997**, *5*, 541.
(54) Tanaka, T. In *Dynamic Light Scattering*; Pecora, R., Ed.; Plenum: New York, 1985.
(55) Wu, C.; Chan, K. K.; Xia, K.-Q. *Macromolecules* **1995**, *28*, 1032.
(56) Wu, C.; Zhou, S. Q. *Macromolecules* **1996**, *29*, 1574.
(57) Heckmeier, M.; Mix, M.; Strobl, G. *Macromolecules* **1997**, *30*, 4454.